Supplementary Material (ESI) for Chemical Communications

A Series of Luminescent Lanthanide-Cadmium-Organic Frameworks with Helical Channels and Tubes

Yan-Qiong Sun,[a] Jie Zhang[a] and Guo-Yu Yang*[,a,b]

State Key Laboratory of Structural Chemistry, Fujian Institute of Research on the Structure of Matter, Chinese Academy of Sciences, Fuzhou, Fujian 350002, China; [b] State Key Laboratory of Rare Earth Materials Chemistry and Applications, Peking University, Beijing 100871, China

Materials and General Details. Commercially available solvents and chemicals were used without further purification. IR spectra were measured as KBr pellets on a Bomem MB102 FT-IR in the range 400-4000 cm^{-1}. The elemental analyses were determined on a Vario EL *III* CHNOS elemental analyzer. Thermalgravimetric data were collected on a Mettler Toledo TGA/SDTA 851^e analyzer in flowing nitrogen at a heating rate of 10 ºC/min. Fluorescence measurements were made with Edingbergh Instrument FL-FS920 TCSPC luminescence spectrometer on powdered crystal material of the compounds.

Synthesis of $LnCd(imdc)(SO_4)(H_2O)_3{\cdot}0.5H_2O$ (Ln = Tb(**1**), Eu(**2**), Dy(**3**), Gd(**4**), Er(**5**), Yb(**6**), Y(**7**), Nd(**8**), Pr(**9**)**.** A mixture of Ln_2O_3 (0.5 mmol) , H_3imdc (2 mmol, 0.312 g), $CdSO_4.8H_2O$ (0.5mmol, 0.385 g) and 10 mL H_2O in a molar ratio of about 1:4:1:1111 (pH = 4) was sealed in a 30 mL stainless steel reactor with teflon liner and heated at 170 ºC for 7 days and then cooled to room temperature. Single crystals suitable for X-ray analyses were recovered by filtration, washed with distilled water and dried in air.

$TbCd(imdc)(SO_4)(H_2O)_3{\cdot}0.5H_2O$ (1) Yield: 83%. Anal. Calcd for $C_5H_8CdN_2O_{11.5}STb$: C, 10.29; H, 1.38; N, 4.80. Found: C, 10.32; H, 1.49; N, 4.37. Main IR absorption bands (cm^{-1}): 3459(m), 1590(s), 1383(s), 1104(s, br), 834(m).

$EuCd(imdc)(SO_4)(H_2O)_3{\cdot}0.5H_2O$ (2) Yield: 74%. Anal. Calcd for $C_5H_8CdN_2O_{11.5}SEu$: C, 10.42; H, 1.40; N, 4.86. Found: C, 10.53; H, 2.10; N, 4.93. Main IR absorption bands (cm^{-1}): 3388(m), 1589(s), 1381(s), 1104(s, br), 832(m).

$DyCd(imdc)(SO_4)(H_2O)_3{\cdot}0.5H_2O$ (3) Yield: 79%. Anal. Calcd for $C_5H_8CdN_2O_{11.5}SDy$: C, 10.23; H, 1.37; N, 4.77. Found: C, 10.19; H, 1.66; N, 4.79. Main IR absorption bands (cm^{-1}): 3410(m), 1589(s), 1383(s), 1106(s, br), 834(m).

$GdCd(imdc)(SO_4)(H_2O)_3{\cdot}0.5H_2O$ (4) Yield: 59%. Anal. Calcd for $C_5H_8CdN_2O_{11.5}SGd$: C, 10.32; H, 1.39; N, 4.81. Found: C, 10.12; H, 1.67; N, 4.76. Main IR absorption bands (cm^{-1}): 3406(m), 1588(s), 1382(s), 1104(s, br), 834(m).

$ErCd(imdc)(SO_4)(H_2O)_3{\cdot}0.5H_2O$ (5) Yield: 81%. Anal. Calcd for $C_5H_8CdN_2O_{11.5}SEr$: C, 10.15; H, 1.36; N, 4.73. Found: C, 10.30; H, 1.45; N, 4.93. Main IR absorption bands (cm^{-1}): 3370(m), 1592(s), 1384(s), 1107(s, br), 835(m).

$YbCd(imdc)(SO_4)(H_2O)_3{\cdot}0.5H_2O$ (6) Yield: 93%. Anal. Calcd for $C_5H_8CdN_2O_{11.5}SYb$: C, 10.05; H, 1.35; N, 4.69. Found: C, 10.22; H, 1.59; N, 4.85. Main IR absorption bands (cm^{-1}): 3369(m), 1593(s), 1382(s), 1108(s, br), 836(m).

$YCd(imdc)(SO_4)(H_2O)_3 \cdot 0.5H_2O$ (7) Yield: 67%. Anal. Calcd for $C_5H_8CdN_2O_{11.5}SY$: C, 11.69; H, 1.57; N, 5.46. Found: C, 10.72; H, 1.79; N, 5.52. Main IR absorption bands (cm^{-1}): 3426(m), 1593(s), 1384(s), 1106(s, br), 834(m).

$NdCd(imdc)(SO_4)(H_2O)_3 \cdot 0.5H_2O$ (8) Yield: 78%. Anal. Calcd for $C_5H_8CdN_2O_{11.5}SNd$: C, 10.56; H, 1.42; N, 4.92. Found: C, 10.72; H, 1.54; N, 5.16. Main IR absorption bands (cm^{-1}): 3389(m), 1579(s), 1380(s), 1102(s, br), 832(m).

$PrCd(imdc)(SO_4)(H_2O)_3 \cdot 0.5H_2O$ (9) Yield: 66%. Anal. Calcd for $C_5H_8CdN_2O_{11.5}SPr$: C, 10.62; H, 1.43; N, 4.95. Found: C, 10.36; H, 1.60; N, 4.99. Main IR absorption bands (cm^{-1}): 3350(m), 1578(s), 1380(s), 1102(s, br), 831(m).

X-ray Crystallography. Suitable single crystals were selected and mounted on a glass fiber. All data were collected at room temperature on a Siemens SMART CCD diffractometer with graphite-monochromated MoKα (λ = 0.71073 Å) radiation in the ω scanning mode at room temperature. An empirical absorption correction was applied using SADABS program. The structures were solved by direct methods and refined by full-matrix least squares on F^2 using the SHELXTL-97 program package. All hydrogen atoms bond N and C were generated geometrically (C-H = 0.93Å, N-H=0.86Å). H atoms associated with water molecules were located in a difference Fourier map and refined with fixed isotropic displacement parameters. Detailed information about the crystal data and structure determination is summarized in Table 1 and CCDC-602025-602033 for **1-9** contain the supplementary crystallographic data for this paper. These data can be obtained free of charge at www.ccdc.cam.ac.uk/conts/retrieving.html [or from the Cambridge Crystallographic Data Centre, 12, Union Road, Cambridge CB2 1EZ, UK; fax: (internet.) +44-1223/336-033; E-mail: deposit@ccdc.cam.ac.uk].

Supporting Tables:

Table 1 Crystal data and structure refinement parameters for compounds **1-9**

Compounds	**1**	**2**	**3**	**4**	**5**
Empirical formula	$C_5H_8CdN_2O_{11.5}STb$	$C_5H_8CdEuN_2O_{11.5}S$	$C_5H_8CdDyN_2O_{11.5}S$	$C_5H_8CdGdN_2O_{11.5}S$	$C_5H_8CdErN_2O_{11.5}S$
Formula weight	583.52	576.55	587.09	581.84	591.85
Crystal system	Monoclinic	Monoclinic	Monoclinic	Monoclinic	Monoclinic
Space group	$P2_1/c$	$P2_1/c$	$P2_1/c$	$P2_1/c$	$P2_1/c$
a/Å	8.6257(7)	8.6305(1)	8.6178(2)	8.6194(6)	8.6197(6)
b/Å	10.4624(7)	10.3517(2)	10.4366(2)	10.4858(6)	10.3244(5)
c/Å	13.8439(10)	13.9069(1)	13.8568(2)	13.8468(11)	13.8885(9)
β/°	101.284(3)	101.688(1)	101.320(1)	101.168(4)	101.714(2)
V/Å^3	1225.20(16)	1216.69(3)	1222.04(4)	1227.79(15)	1210.24(13)
Z	4	4	4	4	4
D_c/g cm^{-3}	3.163	3.148	3.191	3.148	3.248
μ/mm^{-1}	7.701	7.097	8.048	7.326	8.887
F(000)	1092	1084	1096	1088	1104
θ range (°)	3.10-27.48	2.41-25.68	2.41-25.67	2.41-27.47	3.12 -27.48
Tot. no. of data collcd	9101	6468	6409	9269	9095
No. of obsd data ($I>2\sigma(I)$)	2808	2300	2315	2816	2764
Goodness-of-fit on F^2	1.114	1.098	1.077	1.077	1.042
No. of variables	199	199	199	199	199
R_1, wR_2 ($I>2\sigma(I)$)	0.0203, 0.0481	0.0322, 0.0802	0.0218, 0.0539	0.0236, 0.0547	0.0308, 0.0795
CCDC number	602025	602026	602027	602028	602029
Compounds	**6**	**7**	**8**	**9**	
Empirical formula	$C_5H_8CdN_2O_{11.5}SYb$	$C_5H_8CdN_2O_{11.5}SY$	$C_5H_8CdN_2NdO_{11.5}S$	$C_5H_8CdN_2O_{11.5}PrS$	
Formula weight	597.63	513.50	568.83	565.50	
Crystal system	Monoclinic	Monoclinic	Monoclinic	Monoclinic	
Space group	$P2_1/c$	$P2_1/c$	$P2_1/c$	$P2_1/c$	
a/Å	8.6388(1)	8.6115(6)	8.7120(1)	8.7538(1)	
b/Å	10.2591(2)	10.3674(7)	10.5288(2)	10.5445(2)	
c/Å	13.9386(3)	13.8626(13)	13.9024(3)	13.9138(3)	
β/°	101.991(1)	101.547(4)	101.033(1)	101.010(1)	
V/Å^3	1208.37(4)	1212.59(16)	1251.65(4)	1260.67(4)	
Z	4	4	4	4	
D_c/g cm^{-3}	3.285	2.813	3.019	3.980	
μ/mm^{-1}	9.695	6.758	6.036	5.739	
F(000)	1112	988	1072	1068	
θ range (°)	2.41-25.75	3.11-27.48	2.38-25.67	2.37-25.68	
Tot. no. of data collcd	6431	9195	6643	6707	
No. of obsd data ($I>2\sigma(I)$)	2293	2772	2377	2388	
Goodness-of-fit on F^2	1.124	1.091	1.089	1.130	
No. of variables	208	199	199	199	
R_1, wR_2 ($I>2\sigma(I)$)	0.0240, 0.0597	0.0260, 0.0605	0.0232, 0.0559	0.0364, 0.0746	
CCDC number	602030	602031	602032	602033	

Table 2 Geometrical Parameters of Hydrogen Bonds for **1**

D-H	d(D-H)	d(H···A)	<DHA	d(D···A)	A

O(1W)-H(12)	0.85	2.09	141	2.797(8)	O(3W)	
O(1W)-H(12)	0.85	2.35	128	2.943(5)	O(7)	[-x+2, y+1/2, -z+1/2]
O(2W)-H(21)	0.83	2.18	123	2.720(5)	O(8)	[x, -y+3/2, z-1/2]
O(2W)-H(21)	0.83	2.22	147	2.943(9)	O(4W)	[-x+2, y-1/2, -z+1/2]
O(2W)-H(22)	0.94	1.93	140	2.712(5)	O(7)	
O(3W)-H(31)	0.98	2.00	144	2.854(6)	O(5)	[x-1, -y+3/2, z-1/2]
O(3W)-H(32)	0.95	2.19	142	2.994(5)	O(5)	[-x+2, y+1/2, -z+1/2]

Supporting Figures:

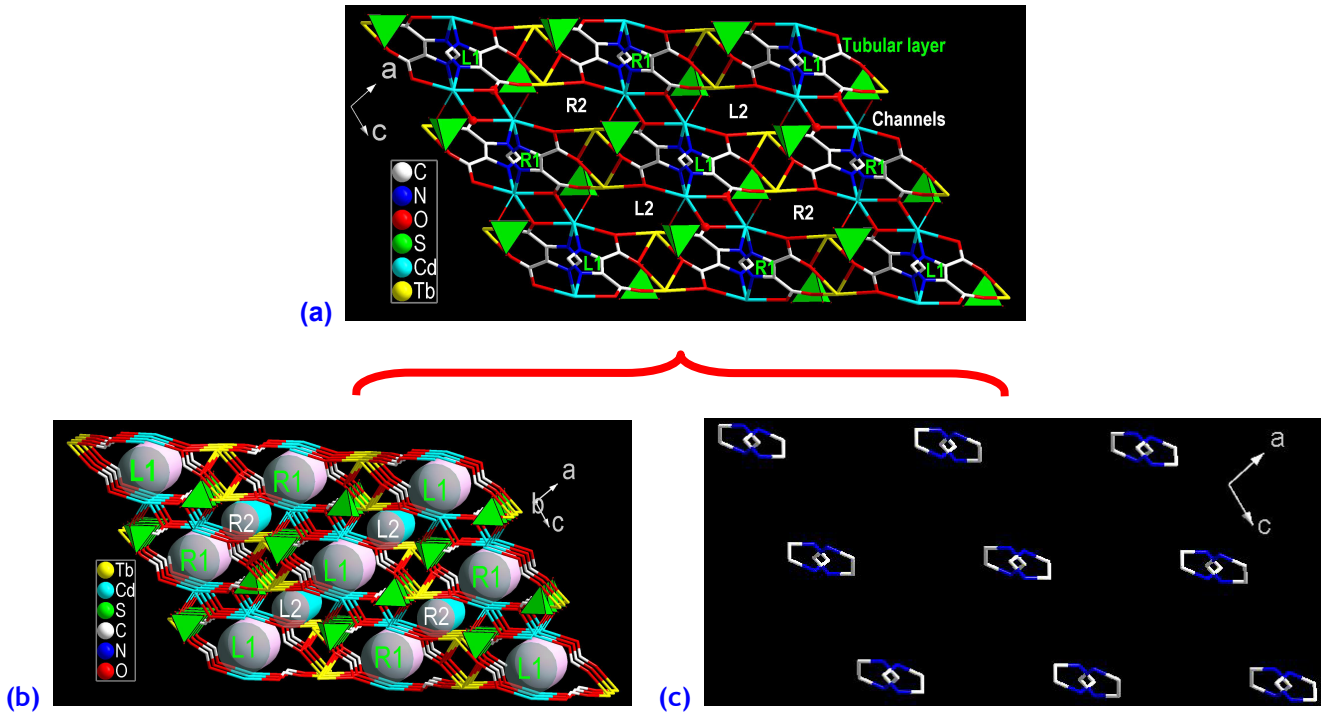

Figure S1. (a) View of the packing structure of **1** down the [010] direction, showing left/right-handed helical tubes (L1/R1) and 1D left/right-handed helical channels (L2/R2). (b) The 3D open-framework constructed from the walls and the fillers in the inner of the tubes in **1** down the [010] direction, showing the helical channels (L2/R2) and the layers made of helical tubes (L1/R1). The water molecules are omitted for clarity. similarly hereinafter. (c) The fillers in **1** along the *b* axis, showing the arrangement of the imidazole rings. L and R: the left- and right-handed helical tubular channels; Color code: cyan, Cd; yellow, Tb; red, O; blue, N, white, C atoms; green polyhedron, SO_4^{2-} anion.

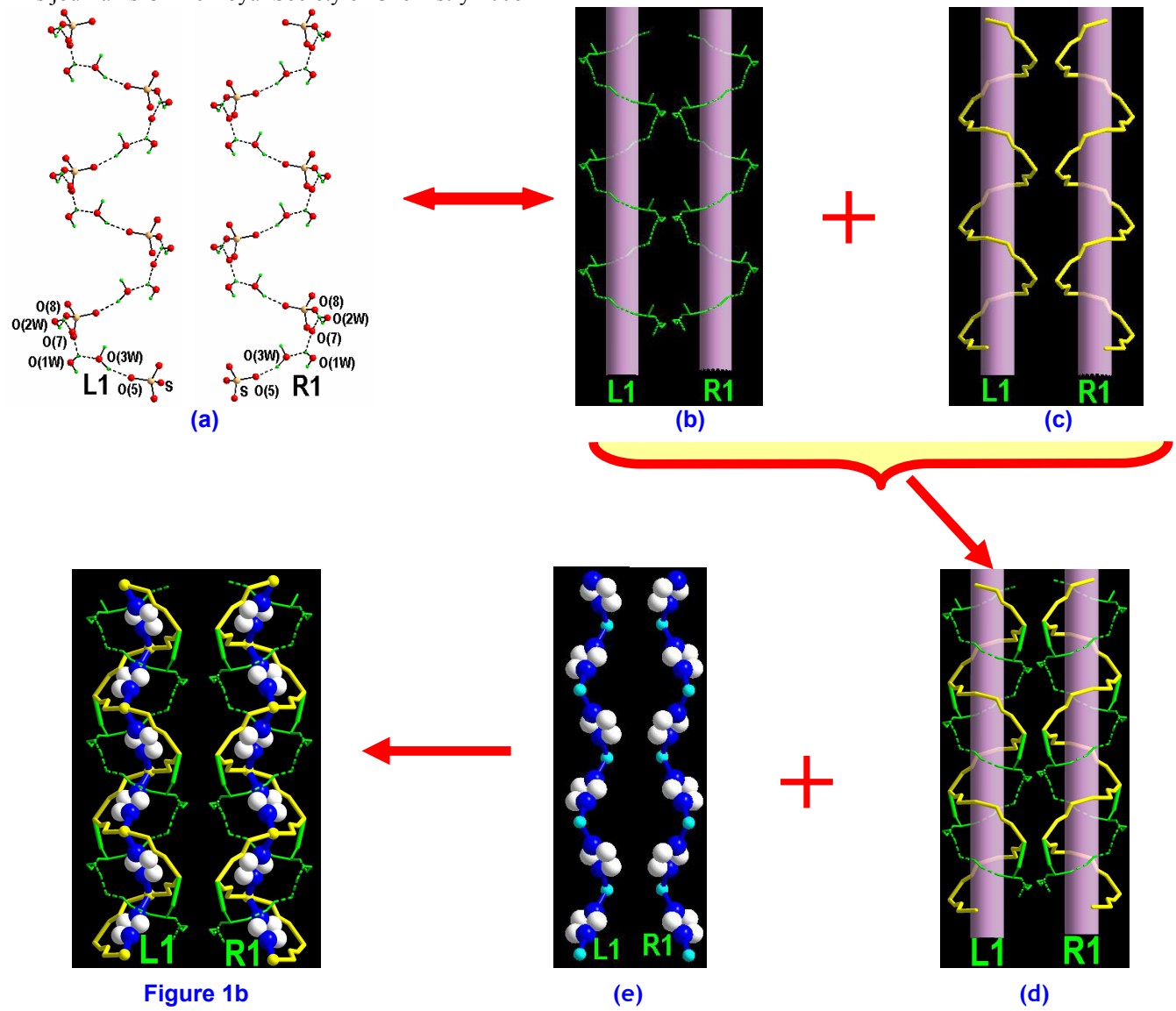

Figure S2. The helical tubular combinations of opposite chirality, showing –Cd–O1–C4–O2–Tb–O3–C5–O4– helical chains being weaved by the similar orientation helical chains, –S–O5···O3W···O1W···O7···O2W···O8– formed *via* H-bonds. (a) Ball-stick representation of the H-bond helical chains of opposite chirality, made of two repeating –S–O5···O3W···O1W···O7···O2W···O8– linkages, along the [010] (L1) and [0-10] (R1) directions. (b) The topology representation of the H-bond helical chains marked green for identification along the [010] (L1) and [0-10] (R1) directions. (c) View of two types of –Cd-O1-C4-O2- Tb-O3-C5-O4- helical chains of opposite chirality marked yellow for identification, showing the similar helical orientation to the H-bond helical chains along the [010] (L1) and [0-10] (R1) directions. (d) View of two types of helical tubes in combination of helical walls made of two kinds of helical chains with similar chirality. (e) Ball-stick representation of the left- and right-handed –Cd-im- helices trapped in inner of the helical tubes along the [010] (L1) and [0-10] (R1) directions. The above three kinds of helices have same helical orientation, L1 and R1, respectively.

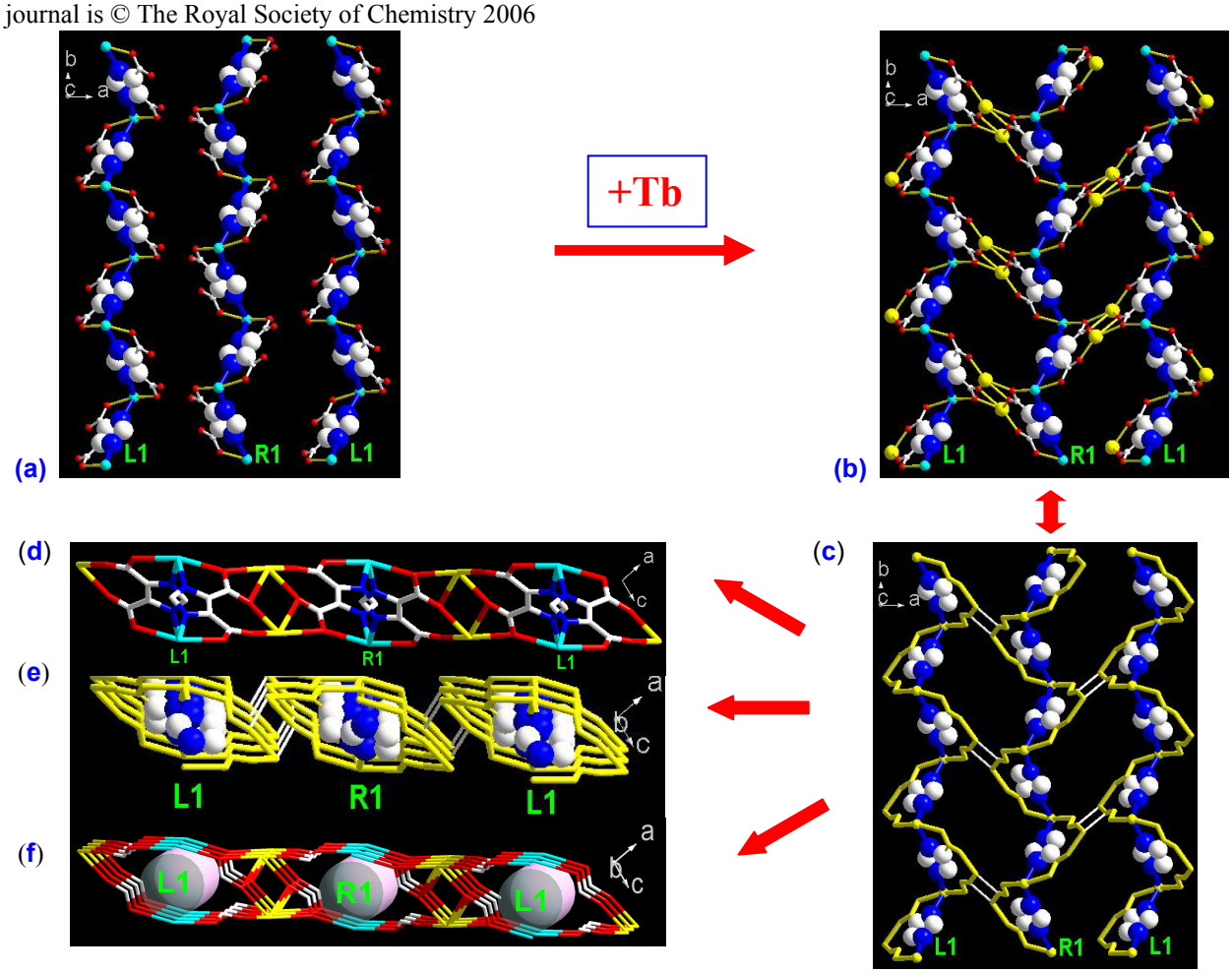

Figure S3. View of the diagrammatic sketch of the construction of the tubular layer **1**. (a) Left- and right-handed –Cd–im– helical chains constructed by imidazole rings of imdc ligands bridged between the Cd^{2+} centers. The water molecules and SO_4^{2-} anions are omitted for clarity, similarly hereinafter. (b) View the 2D tubular layer in the *ab*-plane. Two centro-symmetrically related single-stranded helical chains are bridged by Tb^{3+} ions through bonding to the carboxyls to generate a 2D helical tubular layer in the *ab*-plane. (c) Left- and right-handed –Cd–O1–C4–O2–Tb–O3–C5–O4– helical chains built up from the Tb^{3+} and Cd^{2+} as well as two bridging carboxyl groups, displaying the similar helical orientation to –Cd–im– helice. The –Cd–O1–C4– O2–Tb–O3–C5–O4– helical chains are marked yellow for identification, similarly hereinafter. (d) Stick presentation of the 2D tubular layer along the [010] direction. (e) View of the 2D tubular layer along the approximate [010] direction showing that the –Cd–im– helices as the fillers are trapped in inner of –Cd–O1–C4–O2–Tb–O3–C5–O4– helical tubes. (f) View of the 2D tubular layer along the approximate [010] direction, showing two types of helical tubes (L1/R1). The imidazole rings are omitted for clarity. Color code: cyan, Cd; yellow, Tb; red, O; blue, N, white, C atoms.

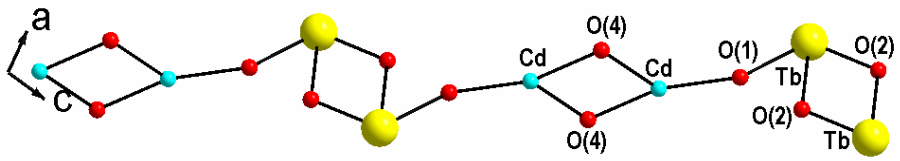

Figure S4. Ball-stick representation of the inorganic heterometallic chain made of Tb_2O_2 and Cd_2O_2 cluster units running along the [101] direction. Color: yellow, Tb; cyan, Cd.

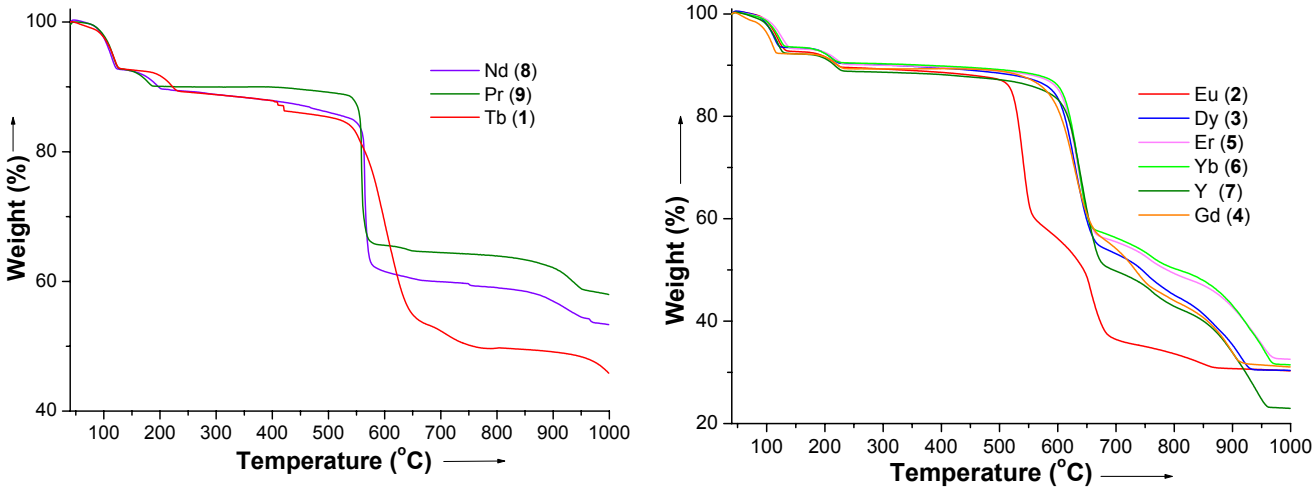

Figure S5. TG curves of $[LnCd(imdc)(SO_4)(H_2O)_3]\cdot 0.5H_2O$ under air atmosphere (10 °C/min).

The thermal stability of $[LnCd(imdc)(SO_4)(H_2O)_3]\cdot 0.5H_2O$ was examined by the TG analysis in dry air atmosphere from 40 to 1000 ºC. The compounds show similar thermal behavior and undergo several steps of weight loss. The lattice water and coordinated waters were gradually lost in the temperature range 40-260 ºC for **1** (calcd/found: 10.81%/10.89%), 40-350 ºC for **2** (calcd/found: 10.93%/11.05%); 40-450 ºC for **3** (calcd/found: 10.73%/10.98%); 40-500 ºC for **4** (calcd/found: 10.83%/11.15%); 40-500 ºC for **5** (calcd/found: 10.65%/11.10%); 40-500 ºC for **6** (calcd/found: 10.55%/10.87%); 40-500 ºC for **7** (calcd/found: 12.28%/12.84%); 40-350 ºC for **8** (calcd/found: 11.08%/11.63%) and 40-545 ºC for **9** (calcd/found: 11.15%/11.99%), respecti- vely. Then the imdc ligands started to decompose and the residue had a composition of $Tb_2O_3\cdot 2CdO$ for **1** (calcd/found: 53.35%/ 52.36%); Eu_2O_3 for **2** (calcd/found: 30.52%/30.29%); Dy_2O_3 for **3** (calcd/found: 31.76%/30.73%); Gd_2O_3 for **4** (calcd/found: 31.15%/31.06%); Er_2O_3 for **5** (calcd/found: 32.31%/32.56%); Yb_2O_3 for **6** (calcd/found: 32.97%/31.36%); Y_2O_3 for **7** (calcd/ found: 21.99%/22.97%); $Nd_2O_3\cdot 2CdO$ for **8** (calcd/found: 52.15%/53.33%) and $Pr_2O_2(SO_4)\cdot 2CdO$ for **9** (calcd/found: 58.95%/ 57.97%), respectively.

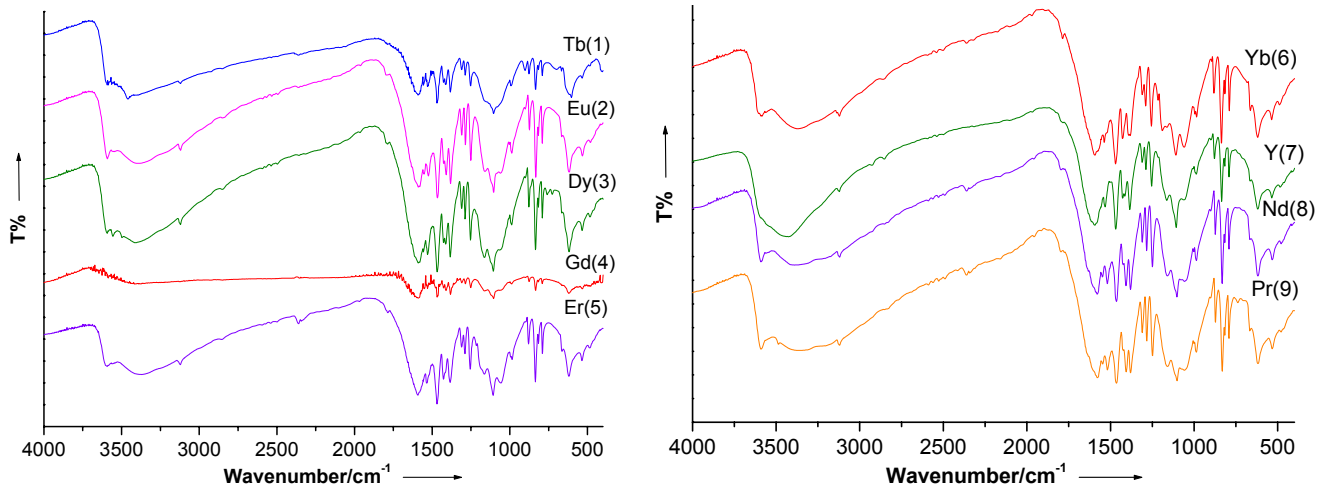

Figure S6. IR spectra of Tb(**1**), Eu(**2**), Dy(**3**), Gd(**4**), Er(**5**), Yb(**6**), Y(**7**), Nd(**8**) and Pr(**9**), respectively.

In the IR spectra, the absence of any strong bands around 1700 cm^{-1} indicates that all carboxylic groups (COOH) are deprotonated. Moreover, they show the asymmetric stretching vibration for the COO^- groups in the regions 1589-1593 cm^{-1} and the symmetric stretching vibration in the regions 1464-1469 cm^{-1}. The strong broad bands at 1102-1107 cm^{-1} can be assigned to the stretching vibrations of SO_4^{2-}.